MAR 5 1998

IUCAA -53/97

October 97

# A study of penetration at the bottom of a convective envelope and its scaling with vertical velocity

IUCAA-53-97

Fermilab Library
0 1160 0061056 2

By

Harinder P. Singh
Ian W. Roxburgh
Kwing L. Chan

| NAME | I D No. | M.S |
|---|---|---|
| | | |

RETURN TO FERMILAB

*Accepted for publication in Astronomy and Astrophysics*

**Inter-University Centre for Astronomy and Astrophysics**

An Autonomous Institution of the University Grants Commission

Preprint Request (Please quote the preprint number)
email : preprn@iucaa.ernet.in
Fax : 0212-350760
Post : IUCAA, Post Bag 4, Ganeshkhind, Pune 411 007, India

A&A manuscript no.
(will be inserted by hand later)

Your thesaurus codes are:
06(02.03.3; 02.08.1; 08.09.3)

ASTRONOMY
AND
ASTROPHYSICS
8.9.1997

# A study of penetration at the bottom of a convective envelope and its scaling with vertical velocity

**Harinder P. Singh[1,2,3], Ian W. Roxburgh[2], and Kwing L. Chan[1]**

[1] Department of Mathematics, The Hong Kong University of Science & Technology, Kowloon, Hong Kong
[2] Astronomy Unit, Queen Mary & Westfield College, University of London, Mile End Road, London E1 4NS, UK
[3] Department of Physics, Sri Venkateswara College, University of Delhi, New Delhi 110 021, India

received date; accepted date

**Abstract.** A number of investigators have proposed a relation between the penetration depth ($\Delta_d$) at the bottom of a convective region and the velocity of the penetrating motions. This may be expressed in a simple form as $\Delta_d \propto V_{zo}^{3/2}$, $V_{zo}$ being the vertical velocity at the bottom of the convection zone. Although the mixing-length theory was not used in these studies, other simplifying assumptions were made. In this paper, we study the general behaviour of motions penetrating into the stable region at the bottom of a convective envelope by numerically solving the full set of Navier-Stokes equations in three dimensions. We compute a series of models which allow us to study the scaling relationship between the penetration distance and the rms vertical velocity.

Key words: convection – hydrodynamics – stars: interiors – stars: structure

## 1. Introduction

A large number of theoretical investigations have been made in the last thirty years to evaluate convective penetration or overshoot in stellar interiors. Because of the complexity of the involved physical processes (see Roxburgh 1997), there has neither been a completely satisfactory treatment of the issue, nor is there a consensus on the magnitude of the overshoot, be it from a convective envelope inwards or a convective core outwards. Even for the best studied case of the Sun, for which high quality oscillation data are available, helioseismic inversion techniques give differing upper limits on the size of overshoot at the bottom of the solar convection zone (Roxburgh 1996). On the other hand, two and three-dimensional simulations of compressible convection, with a view to study overshoot, have recently been attempted (Roxburgh and Simmons 1993; Hurlburt et al. 1994; Singh et al. 1994, 1995, 1996; see also Nordlund & Stein 1996; Muthsam et al. 1995). Compared to convection zone of the sun, the convection zones in these simulations are shallower with low density contrasts. As $F/\rho \propto V_z{}^3$ in a convection zone, where $F$ is the total flux, such configurations generate comparatively large flow velocities and hence tend to over-estimate the extent of penetration or overshoot. Neglect of rotational effects could also be responsible. Since we are still far away from having the desired computing power that will allow us to simulate the solar convection zone, the remedy is to find some scaling relationships between physical quantities of interest which could then be applied to the Sun.

Of particular interest, in the present context, are the calculations of Schmitt et al. (1984) and Zahn (1991). Schmitt et al. adopted a semitheoretical approach, derived originally for the Earth's atmosphere, to study convective penetration in stars. They considered the equations of motions for buoyant plumes and applied them to the penetration problem in the Sun. The equations were solved numerically to obtain a simple scaling relation for penetration in terms of the initial vertical velocity $V_{zo}$ (velocity at the bottom of the convection zone) and a filling factor $f$ (the fraction of the area occupied by the plumes) as $V_{zo}^{3/2} f^{1/2}$. If initial velocities predicted by the mixing length theory are used, their results predict an almost adiabatically stratified region, a few-tenths of a pressure scale height in extent, below the solar convection zone. Zahn (1991) treated the problem analytically, basing it on scaling arguments and explained why the depth of the nearly adiabatic penetration region should scale as $V_{zo}^{3/2}$.

Numerical simulations of turbulent compressible convection have been attempted by various groups. The first attempt to find scaling relationships within a stellar-type convection zone was made by Chan & Sofia (1989). They found scaling relationships between the rms fluctuations of pressure, density, specific entropy, temperature, and velocity. These scaling relationships have been successfully employed to compute equilibrium models of the Sun and $\alpha$ Centauri by replacing the mixing length theory of convection (Lydon et al. 1992, 1993). The relations were further examined by Singh & Chan (1993) and Chan & Sofia (1996).

Simulations of penetrative convection have been performed in two dimensions with different objectives by Roxburgh & Simmons (1993), Hurlburt et al. (1994), and Freytag et al. (1996). Hurlburt et al. gave scaling laws relating the penetration distance with the relative stability of the unstable to the stable zone. Three- dimensional simulations have been performed to study the behaviour of penetrative convection above and below a convection zone by Singh et al. (1994, 1995). A number of models were computed in each case and it was observed that the penetration distance above a convection zone

*Send offprint requests to*: H.P.Singh at qmw.ac.uk

**Fig. 1.** Some geometrical and physical parameters of the configuration

was proportional to the maximum vertical velocity of the convective motions and this distance increased with the factor $F_b/\rho_{czt}$, where $F_b$ denotes the input flux and $\rho_{czt}$ the density at the top of the convection zone. The penetration distance below a convection zone was found to decrease as the stability of the lower stable region was increased, a behaviour which was also observed in the two- dimensional simulations of Hurlburt et al.

In this paper we study the behaviour of penetrative convection below a deep stellar- type convective envelope by computing a series of models with various input flux values. We also examine the scaling relationship $\Delta_d \propto V_{zo}^{3/2}$ between the vertical velocity of the flows and the penetration distance as given by Schmitt et al. (1984) and Zahn (1991). In the next section we provide essential features of our models and the parameters of the simulation. In Sect. 3 we report detailed results of our computations in terms of time and space-averaged quantities. Important conclusions based on the results are presented in Sect. 4.

## 2. Model Parameters

A detailed discussion of the input physics and the numerical parameters of the simulation has been given in Singh et al. (1995) (hereafter referred to as SRC95). We provide here some necessary details of the present set of calculations.

The fluid is an ideal gas with $\gamma = 5/3$ and is contained in a rectangular box with the two equal horizontal sides 1.5 times the height ($z$). A mesh of 35 points each in the two horizontal directions and 51 points in the vertical occupies this rectangular domain. While the mesh points in the horizontal directions are equally spaced, the spacing in the vertical direction decreases smoothly with height. The top and bottom of the box are impenetrable and stress free while the sides are periodic. The temperature at the top is kept constant while a fixed energy flux $F_b$ is imposed at the bottom.

The three (stable-unstable-stable) layer configuration for the simulation is generated by controlling the conductivities of the diffusive flux. The initial distribution of the gas is polytropic and the polytropic indices from the top down are 1.5, 1.5, and 2. In Fig. 1, we have shown the location of the three

**Fig. 2a-b.** The depth distributions of time and space (horizontal) averaged (a) kinetic energy, and (b) enthalpy fluxes for various cases

layers along with the temperature, pressure, and density contrasts between the top and the bottom. The variables are made dimensionless by scaling so that the initial temperature, pressure, density, and the total depth of the domain all equal 1 at the top. The velocities are scaled to $(p_t/\rho_t)^{1/2}$ and the scaling for various fluxes including the input flux is $(p_t\, V_t)$. The subscript 't' refers to the initial values of the quantities at the top of the domain. In all the cases that we study for the penetration at the bottom of the unstable layer, the lower stable layer extends to a height of 0.4 from the bottom and contains around 1.2 pressure scale heights (p.s.h.). The unstable region is embedded between the two stable layers and contains 5.4 p.s.h. A thin stable layer at the top separates the convectively unstable region from the top boundary.

The energy budget of the system is described in terms of a total flux made up of four fluxes : the enthalpy flux ($F_e$), the flux of kinetic energy ($F_k$), the diffusive flux ($F_d$), and the viscous flux ($F_v$). The three- layer configuration is evolved with time till the the sum of these four fluxes is almost equal to the input flux $F_b$ at all depths. Once the fluid is thermally relaxed, the equations are integrated for some more time and the combined temporal and spatial (horizontal) means of various physical quantities are computed. We have considered four separate configurations in this manner, corresponding to four different values of the input flux $F_b$. All other parameters are the same for the four models (SRC95).

**Fig. 3.** The extent of penetration for different input fluxes $F_b$. The circles correspond to penetration depths where the kinetic energy flux is 5% of its value at the bottom of the convection zone

**Fig. 4.** The superadiabatic gradient plotted against depth for input flux 0.0625. The kink near the interface of the unstable- lower stable layer may be due to low resolution there

**Table 1.** Penetration below the convective region

| Input Flux $F_b$ | $V_z''(max)$ | $V_{zo}''$ | Penetration $\Delta_d$ | Penetration $\Delta_p$ (in p.s.h.) |
|---|---|---|---|---|
| 0.1875 | 0.330 | 0.119 | 0.275 (0.233)* | 0.88 (0.77) |
| 0.125 | 0.291 | 0.103 | 0.233 (0.208) | 0.77 (0.70) |
| 0.0625 | 0.232 | 0.081 | 0.160 (0.156) | 0.55 (0.54) |
| 0.03125 | 0.186 | 0.062 | 0.112 (0.127) | 0.40 (0.45) |

* the numbers in parentheses correspond to depth where $F_k$ has fallen to 5% of its value at the lower interface

## 3. Results

Fig. 2a shows the distribution of the average flux of kinetic energy, $(1/2)\rho V^2 V_z$, with depth for the four cases corresponding to four different flux values. The unstable region is marked by a line extending from a depth of 0.02 to 0.6 from the top. For all the flux values, the kinetic energy flux ($F_k$) in this region remains negative and drops to zero not at the (unstable-lower stable layer) interface, but a considerable distance into the lower stable layer. The peak $F_k$ value corresponds to -0.111 for the case of input flux $F_b$ equal to 0.1875. The peak $F_k$ for input flux 0.03125 is -0.018. Hence, while the input flux has changed by a factor of 6, from 0.1875 to 0.03125, peak kinetic energy flux has fallen by an almost similar amount, by a factor of 6.17. In all the four cases, this peak kinetic energy flux $F_k$ is around 60% of the input flux $F_b$. The enthalpy flux $F_e$ is positive in the unstable region (Fig. 2b).

As has been done in some previous studies (Hurlburt et al. 1994; SRC95), we use the profile of the flux of kinetic energy to estimate the extent of penetration into the lower stable layer at the bottom of the convectively unstable region. We define the penetration distance ($\Delta_d$) to be the length of the region between the interface of the unstable- lower stable layer and the depth where the kinetic energy flux has fallen to $10^{-3}$. To achieve this, we perform polynomial interpolation to obtain the values of $F_k$ between the grid points. The penetration distances for our four cases are given in Table 1. The result is also plotted in Fig. 3. It may be seen that the penetration distance increases almost linearly with the input flux $F_b$. $\Delta_d$ is 0.275 corresponding to 0.88 p.s.h. for the case with the largest input flux of 0.1875. It has decreased by a factor of 2.2 to 0.40 p.s.h. while the input flux has decreased by a factor of 6 (to 0.03125).

For the case with the highest input flux $F_b = 0.1875$, the penetration distance is 0.275 while the extent of the lower stable layer is 0.4. It is possible that the lower solid boundary is affecting the flows in this case leading to an underestimation of the penetration distance for this flux value.

Since the computation of penetration distance in the above manner may seem arbitrary, we employ one more criterion, which has been used in some earlier studies (Hurlburt et al. 1994; SRC95) and is also based on the flux of kinetic energy. We compute the penetration depth to where $F_k$ is 5% of its value at the interface of the unstable- lower stable layer. The values obtained with this definition of penetration distance are given in parentheses in Table 1. For the input flux 0.1875, we find $\Delta_d = 0.233$ which is about 15% lower than the one found with our earlier criterion. For the lowest flux of 0.03125, $\Delta_d$ is 0.127 instead of 0.112.

The penetration region in our simulations is nearly adiabatic as expected for a configuration with a low relative stability parameter S which is equal to 1 in our case (Hurlburt et al. 1994; SRC95). Furthermore, the local Peclet number is still greater than unity in the penetration region thereby establishing a nearly adiabatic stratification and extending the convection zone into the subadiabatic domain (Fig. 4).

In order to study the relationship between the vertical velocity and the penetration distance, we have computed the average root- mean- square (rms) vertical velocities ($V_z''$) of the four models. The distributions of $V_z''$ over the vertical domain for the four input fluxes are shown in Fig. 5. The maximum values of the rms vertical velocities ($V_z''(max)$) and their values at the bottom of the convection zone ($V_{zo}''$) are given in Table 1. In all the cases the velocities peak at a depth of around 0.055 from the top and fall to about 35% of their peak value at the depth 0.6, the bottom of the convective layer.

Before examining our results further, let us consider the relation obtained by Schmitt et al. (1984) using the phenomenological plume equations :

$$\Delta_d \approx V_{zo}^{3/2} f^{1/2} . \quad (1)$$

**Fig. 5.** The rms vertical velocities ($V_z''$) plotted against depth for the four cases

**Table 2.** Values of the expressions on the left and the right hand side of Eq.(3) for various flux values taken in pairs

| Case $(F_b(1), F_b(2))$ | $\frac{\Delta_d(F_b(1))}{\Delta_d(F_b(2))}$ | $\frac{V_{zo}''^{3/2}(F_b(1))}{V_{zo}''^{3/2}(F_b(2))}$ |
|---|---|---|
| (0.1875, 0.125) | 1.18 (1.19)* | 1.24 |
| (0.1875, 0.0625) | 1.72 (1.82) | 1.78 |
| (0.1875, 0.03125) | 2.46 (2.49) | 2.66 |
| (0.125, 0.0625) | 1.46 (1.54) | 1.43 |
| (0.125, 0.03125) | 2.08 (2.10) | 2.14 |
| (0.0625,0.03125) | 1.43 (1.36) | 1.49 |

* the values in parentheses in the second column represent the ratios of penetration distances corresponding to where $F_k$ is 5% of its value at the unstable- lower stable interface

Zahn (1991) used some simplified modeling and obtained the following result for the case of a smooth conductivity profile with depth :

$$\frac{\Delta_d}{H_p} = V_{zo}^{3/2}(cf)^{1/2}\left[\frac{3}{2}\,g\,Q\,K\,\chi_p\,\nabla_{ad}\right]^{-1/2}, \qquad (2)$$

where $H_p$ is the pressure scale height, $g$ is the local gravity, $Q$ is the expansion coefficient at constant pressure, $\chi_p = (\partial \ln K_R/\partial \ln P)_{ad}$, $K$ is the thermal diffusivity, and $\nabla_{ad} = (\partial \ln T/\partial \ln P)_{ad}$. The quantity $c$ measures the asymmetry of the flow and is related to the triple moment of the velocity as

$$cf = \frac{\overline{V_z(V_x^2 + V_z^2)}}{(\overline{V_z^2})^{3/2}}.$$

As may be noticed, Eq.(2) is in agreement with Eq.(1).

Since we have used a piecewise conductivity (cf. SRC95), we make use of Eq.(1) to study our results further. Also, since $f$ is an unknown, we study a modified Eq.(1) of the form

$$\frac{\Delta_d(F_b(1))}{\Delta_d(F_b(2))} = \frac{V_{zo}''^{3/2}(F_b(1))}{V_{zo}''^{3/2}(F_b(2))}. \qquad (3)$$

The left hand side of Eq.(3) represents ratio of penetration distances corresponding to any two flux values and the right hand side represents the ratio of the rms vertical velocities raised to the power 3/2 for these two flux values. By taking our four flux values in pairs, we obtain six set of values for the left and the right hand sides of Eq.(3). The values are given in Table 2.

**Fig. 6.** Relationship between the penetration distance and the rms vertical velocity from numerical simulations. The solid diagonal line represents Eq.(3). Circles represent ratios of penetration distance computed when the kinetic energy flux has fallen to 5% of it value at the interface of the unstable and the lower stable layer

In Fig. 6 we have plotted the factor on the right hand side of Eq.(3) against the ratio of the penetration distances (the l.h.s. of Eq.(3)). Eq.(3) is represented by the diagonal line. The values from the simulations The points lie close to the diagonal confirming that $\Delta_d \propto V_{zo}^{3/2}$ is a good approximation.

## 4. Conclusions

We have simulated the behaviour of turbulent compressible convection penetrating into stable layer at the bottom of a stellar-type convective envelope. Four models were computed corresponding to four different values of the input flux $F_b$, which is imposed at the lower boundary of the numerical box. We have seen that a larger input flux implies more vigourous convection with larger velocities. The depth of the nearly adiabatic penetration region, computed from the profile of kinetic energy flux $F_k$, has been found to increase with the increase in the input flux.

We have also examined the relationship between the penetration distance ($\Delta_d$) and the root-mean-square vertical velocity by means of Eq.(3). We find that $\Delta_d \propto V_{zo}^{3/2}$ is a valid approximation of the relationship between the two quantities as proposed earlier by Schmitt et al.(1984) and Zahn (1991).

We have also observed (cf. Table 2 and Fig. 6) that for the larger flux value (0.1875), our configuration slightly underestimates the penetration depth. It is desirable, therefore, to have a broader lower stable layer for large flux values so that the boundary effects are minimal. It is also desirable to have a conductivity profile which is continuous, rather than piecewise, to enable examination of Eq.(2) in greater detail. Such Computations will, however, be much more expensive to perform. We hope to address some of these issues in future.

*Acknowledgements.* This work is supported in part by the PPARC, U.K., Research Grant Council, Hong Kong and the Indian Space Research Organisation (grant 10/2/247). PPARC grant GR/K 09526 provided the computer time on the Cray J90 at the Atlas Centre. We also thank the Director, IUCAA, Pune for providing time on the DEC 3000/800S on which initial models were tested.

## References

Chan, K. L., Sofia, S. 1989, ApJ, 336, 1022

Chan, K. L., Sofia, S. 1996, ApJ, 466, 372

Freytag, B., Ludwig, H. G., Steffen, M. 1996, A&A, 313, 497

Hurlburt, N. E., Toomre, J., Massaguer, J. M., Zahn, J.-P. 1994, ApJ, 421, 245

Lydon, T. J., Fox, P. A., Sofia, S. 1992, ApJ, 397, 701

Lydon, T. J., Fox, P. A., Sofia, S. 1993, ApJ, 403, L79

Muthsam, H. J., Gob, W., Kupka, F., Leibich, W., Zochlin, J. 1995, A&A, 293, 127

Nordlund A., Stein, R. F. 1996, in Stellar Evolution: What should be done ? Proceedings of the 32nd Liege Colloquium, Eds. Noels, A., Fraipont-Car, D., Gabriel, M., Grevesse, N., Demarque, P., 75

Roxburgh, I. W. 1996, Bull. Astr. Soc. India, 24, 89

Roxburgh, I. W., Simmons, J. 1993, A&A, 277, 93

Roxburgh, I. W. 1997, SCORe Proceedings, eds. Pijpers, F., Christensen-Dalsgaard, J., 23

Schmitt, J. H. M. M., Rosner, R., Bohn, H. U. 1984, ApJ, 282, 316

Singh, H. P., Chan, K. L. 1993, A&A, 279, 107

Singh, H. P., Roxburgh, I. W., Chan, K. L. 1994, A&A, 281, L73

Singh, H. P., Roxburgh, I. W., Chan, K. L. 1995, A&A, 295, 703 (SRC95)

Singh, H. P., Roxburgh, I. W., Chan, K. L. 1996, Bull. Astr. Soc. India, 24, 281

Zahn, J.-P. 1991, A&A, 252, 179

This article was processed by the author using Springer-Verlag TEX A&A macro package 1991.

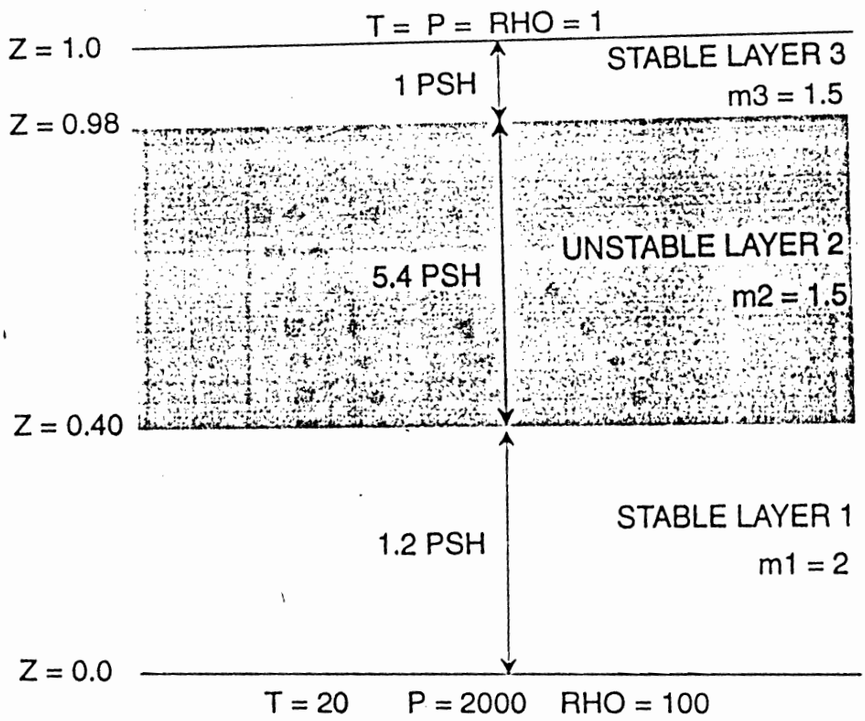
T = P = RHO = 1
Z = 1.0
STABLE LAYER 3
m3 = 1.5
1 PSH
Z = 0.98
UNSTABLE LAYER 2
m2 = 1.5
5.4 PSH
Z = 0.40
STABLE LAYER 1
m1 = 2
1.2 PSH
Z = 0.0
T = 20 P = 2000 RHO = 100

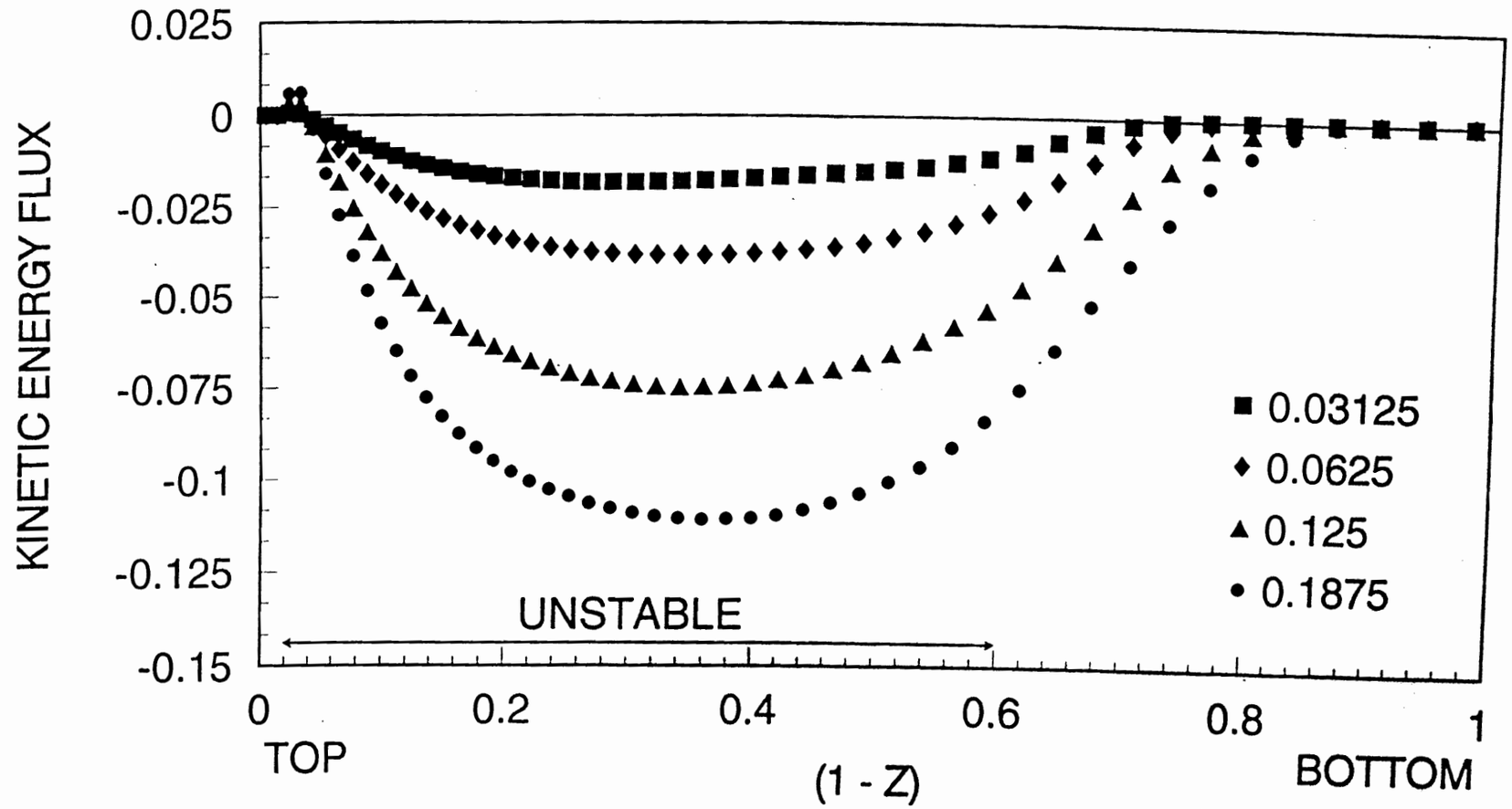
KINETIC ENERGY FLUX
0.025
0
-0.025
-0.05
-0.075
-0.1
-0.125
-0.15
0
0.2
0.4
0.6
0.8
1
TOP
(1 - Z)
BOTTOM
UNSTABLE
0.03125
0.0625
0.125
0.1875

Fig 2a

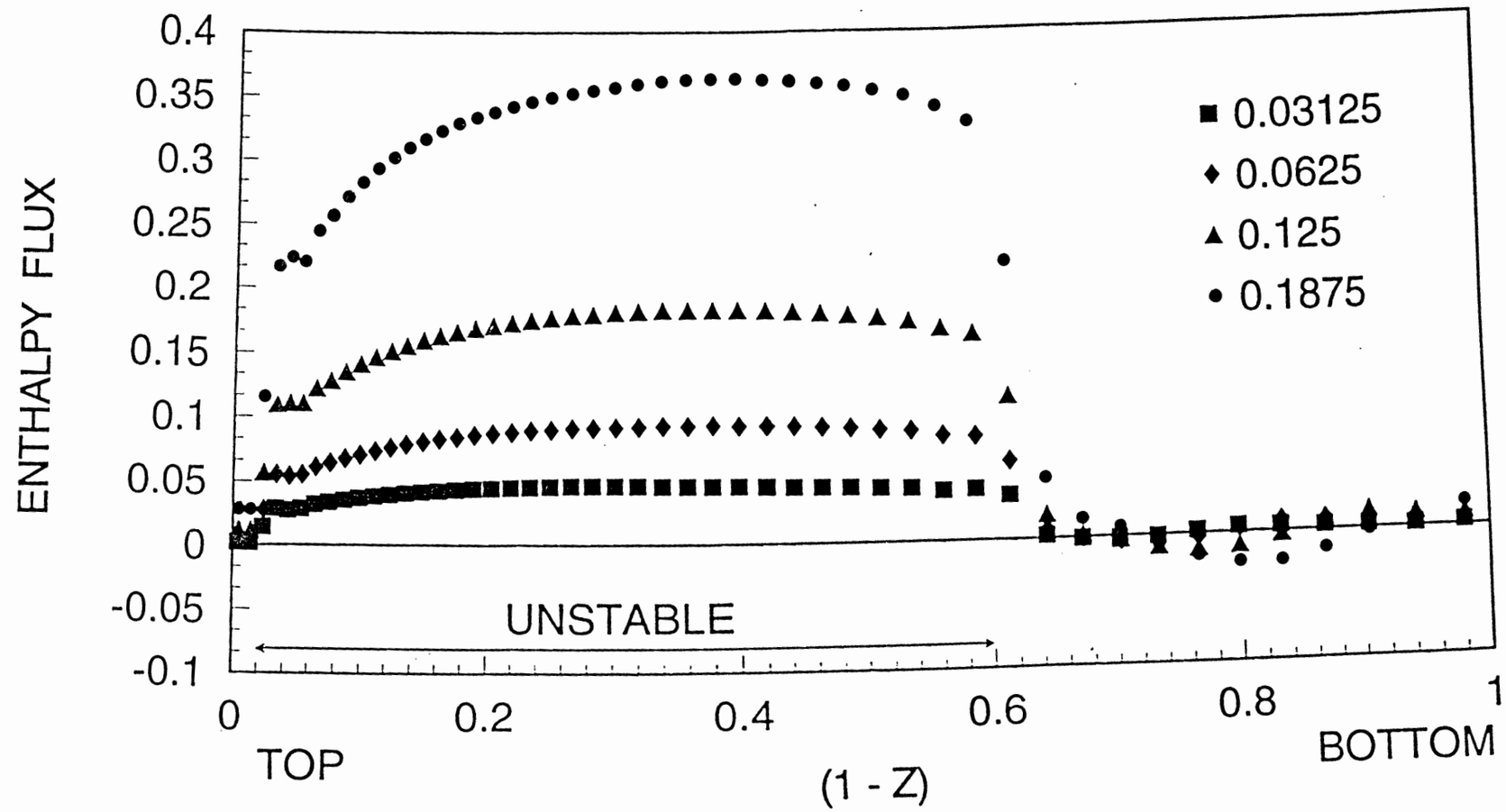
ENTHALPY FLUX
0.4
0.35
0.3
0.25
0.2
0.15
0.1
0.05
0
-0.05
-0.1
0.03125
0.0625
0.125
0.1875
UNSTABLE
0
0.2
0.4
0.6
0.8
1
TOP
BOTTOM
(1 - Z)

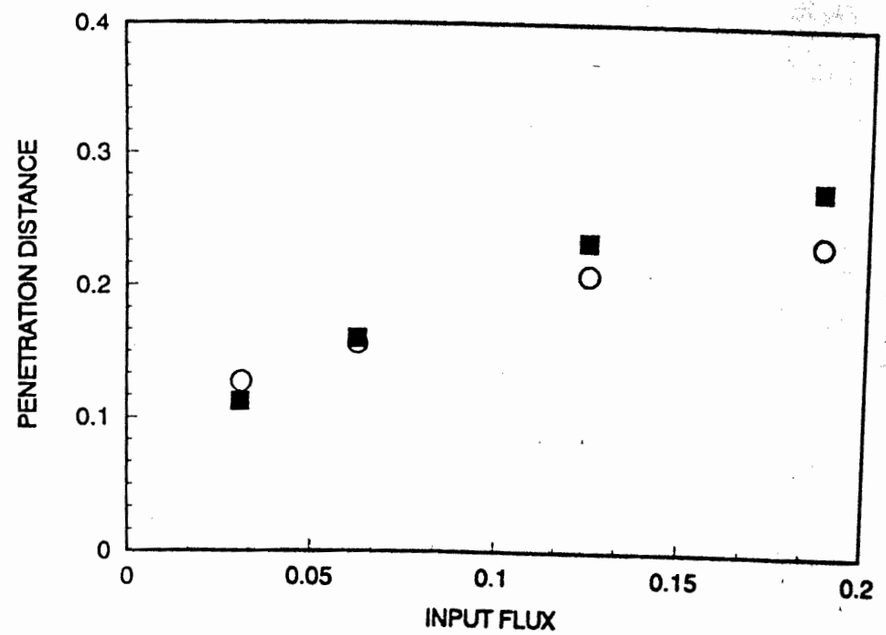
PENETRATION DISTANCE
0.4
0.3
0.2
0.1
0
0
0.05
0.1
0.15
0.2
INPUT FLUX

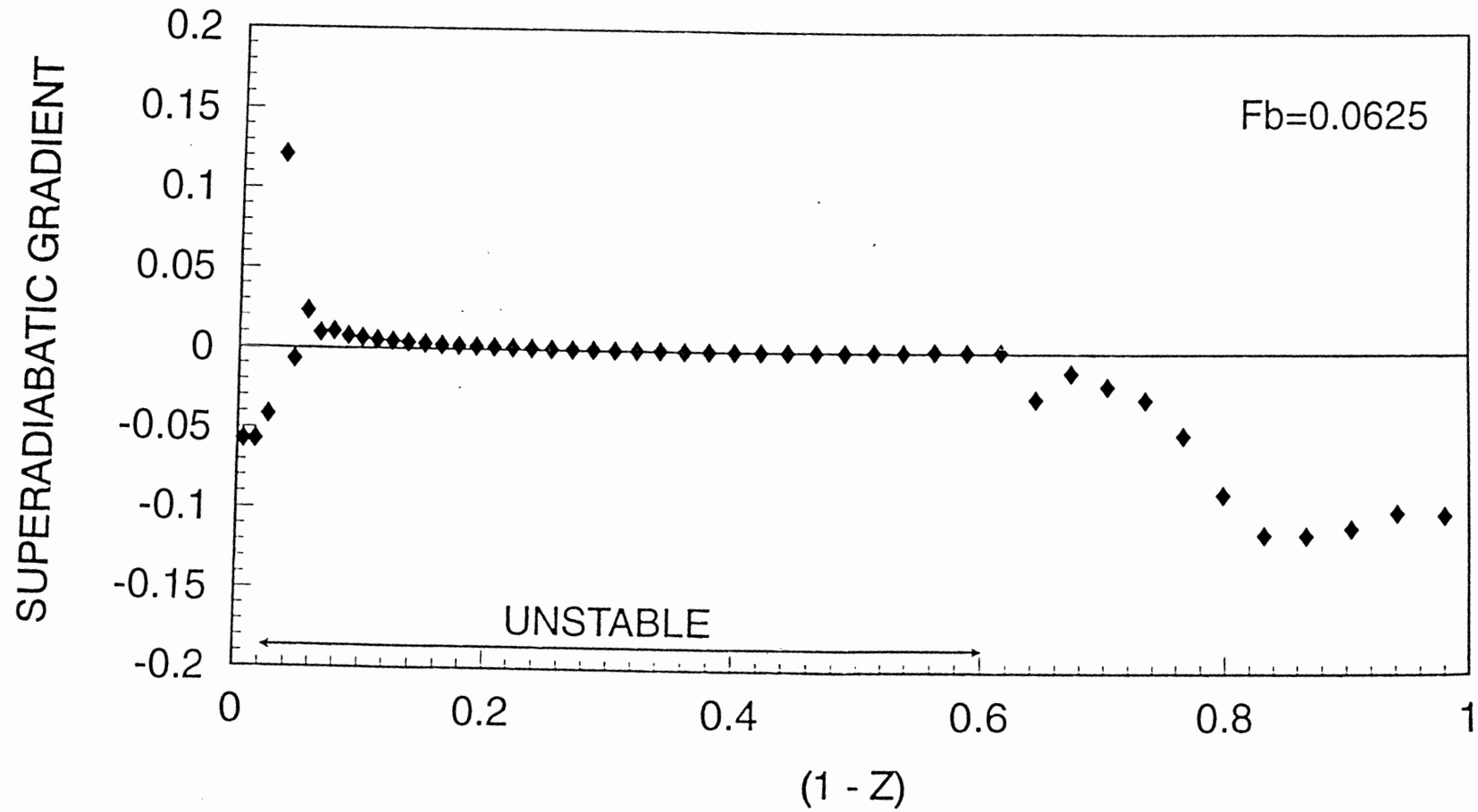
SUPERADIABATIC GRADIENT
0.2
0.15
0.1
0.05
0
-0.05
-0.1
-0.15
-0.2
Fb=0.0625
UNSTABLE
0
0.2
0.4
0.6
0.8
1
(1 - Z)

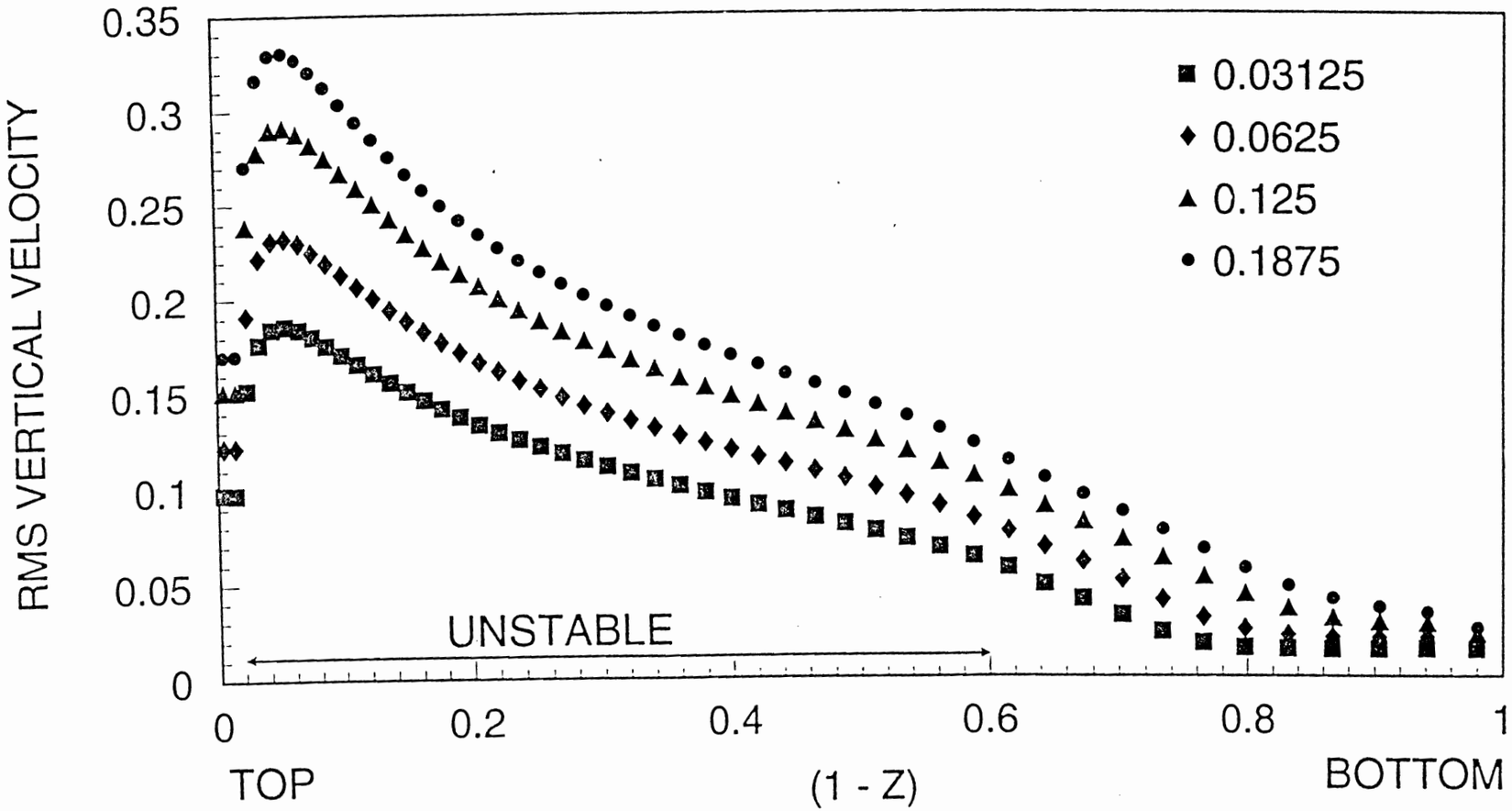
RMS VERTICAL VELOCITY
0.35
0.3
0.25
0.2
0.15
0.1
0.05
0
0.03125
0.0625
0.125
0.1875
UNSTABLE
0
0.2
0.4
0.6
0.8
1
TOP
(1 - Z)
BOTTOM